Permeability and Solute Retention Properties of Conventional and Polymer-Treated Prehydrated GCLs

PERMEABILITY AND SOLUTE RETENTION PROPERTIES OF CONVENTIONAL AND POLYMER-TREATED PREHYDRATED GCLs

Francesco Mazzieri[1], Davide Bernardo[2]

[1]Department SIMAU, Marche Technical University, Via Brecce Bianche,12 , Ancona 60131, Italy; e-mail: f.mazzieri@staff.univpm.it., corresponding author

[2]Department SIMAU, Marche Technical University, Via Brecce Bianche,12 , Ancona 60131, Italy; e-mail: d.bernardo@pm.univpm.it.

Keywords: Geosynthetic Clay Liners, hydraulic conductivity, heavy metals, polymers

ABSTRACT: Polymer treatment is an increasingly adopted approach to mitigate the impact of aggressive liquids on GCLs' hydraulic performance. Dense PreHydrated (DPH) GCLs are particular products that combine polymer treatment, prehydration and densification to improve the overall containment performance. The paper investigated the saturated hydraulic conductivity, *k*, and heavy metals retention in a conventional GCL and a DPH GCL. Both materials were permeated first with water and then with synthetic solution containing Zn, Cu, Pb, also with the purpose to extend a previous study were a solution of the same solutes at higher concentrations had been used. The *k* of the conventional GCL increased by one order of magnitude with respect to water upon permeation with the synthetic solution. The solutes were partly retained and the increase in *k* was associated with the breakthrough of solutes. Upon permeation with the same solution, the *k* of the DPH GCL decreased by a factor 1.6 with respect to water. No significant breakthrough of metals was observed, despite the considerably longer test duration. Under the adopted testing conditions, owing to polymer amendment and densification the hydraulic performance and solute retention properties of the DPH GCLs were superior to the conventional GCL.

1. Introduction

Geosynthetic Clay Liners, (GCLs) consisting of a thin layer of bentonite clay incorporated between two geotextiles or glued to a geomembrane have been widely used as hydraulic and pollutant barriers (Bouazza, 2002). The content of sodium montmorillonite is the key factor for the characteristically low hydraulic conductivity of hydrated bentonite. GCLs are also employed in applications where metal-rich leachates and liquors must be contained (Bouazza, 2010, Liu et al., 2013).

Heavy metals such as Pb, Cu and Zn are commonly found in leachates of MSW and HW landfills (Rowe et al., 2004) as well as in other containment applications such as mine water treatment systems (Lange et al., 2007; Lange et al., 2010). The hydraulic conductivity performance and the retention capacity of GCLs in the presence of metal-rich permeant liquids are thus of interest for these installations. Lake et al. (2007) performed permeability and diffusion tests using a needle-punched GCL and aluminum-rich solutions. The GCL was prehydrated with water and maintained k lower than 5×10^{-11} m/s upon permeation with the aluminum solution. Aluminum attenuation was observed, as a result of cation exchange and precipitation of Al-minerals. Batch tests confirmed the high rate of aluminum uptake to the sodium bentonite, as well as nonlinear sorption behavior. Lange et al. (2007) investigated the retention of metals in a needle-punched GCL permeated with two synthetic mining leachates (ARD, acid rock drainage, and GMT, gold mine tailings). The hydraulic conductivity remained of the same order of magnitude (from 1.6×10^{-11} m/s to 5×10^{-11} m/s) or increased to 1.3×10^{-10} m/s after 21 pore volumes of permeation with the GMT and ARD solutions, respectively. The GCL tested showed strong attenuation for a large number of metals and metalloids present in the synthetic leachates, which was ascribed to cation exchange, precipitation or co-precipitation.

Benson et al. (2008) conducted permeability tests on two needle-punched GCLs from different manufactures (GCL-A and GCL-B), using an alumina processing residue. Both prehydrated (with tap water) and nonprehydrated tests were performed. When permeated with leachate, GCL-A became more permeable than

during permeation with water by a factor of 500, whereas the *k* dropped drastically for GCL-B, probably as a result of precipitation of aluminum salts. Nonprehydrated GCLs were 600-800 times more permeable than the prehydrated GCLs when permeated with the same leachate.

Shackelford et al. (2010) evaluated the hydraulic conductivity of two GCLs, a standard sodium bentonite GCL and a contaminant resistant GCL, considered as a liner component for a mine tailings impoundment. The two GCLs were permeated with groundwater and two electrolyte solutions, a process water (PW) and a simulated leachate (SL) with chemical compositions consistent with those expected during operation. Test results showed that both PW and SL had a significant adverse impact on the hydraulic performance of both GCLs. The mean values of *k* based on permeation with either PW or SL relative to the values of *k* based on permeation with ground water ranged from a factor of 200 to a factor of 7600. Unexpectedly, the contaminant-resistant GCL performed worse than the standard GCL.

Naka et al. (2019) investigated the swell index, hydraulic conductivity and heavy metal attenuation of a GCL containing powdered Na-bentonite against six artificial ARDs with an approximate pH of 3 and different metal concentrations (electrical conductivity, EC, ranging between 75 and 1000 mS/m; ionic strength ranging between 8 and 400 mM). The hydraulic conductivity of the GCL permeated with distilled water was 1.2×10^{-11} m/s, falling in the range of 7.9×10^{-12} to 1.1×10^{-10} m/s when prehydrated with distilled water and permeated with ARDs. Ion exchange and metal precipitation appeared to be the main mechanisms controlling the attenuation on the bentonite. From the overall results, the tested GCL showed acceptably low hydraulic conductivity and the potential to attenuate heavy metals present in ARDs.

Gupt et al.(2020a; 2020b) evaluated by batch tests at controlled pH of 5 the adsorption capacity for Pb of bentonite (B) and bentonite amended with fly-ash (FA) for landfill liners applications. The adsorption of Pb to bentonite and FA admixtures was strongly nonlinear and well modelled by Langmuir and Freundlich isotherms. They reported that the hydraulic conductivity of B-FA mixtures is in the range $10^{-10}\div10^{-12}$ m/s, showing the feasibility of B-FA mixtures as a replacement for conventional B-sand mixtures in landfill liner applications.

Bentonites amended with polymers (Ashmawy et al., 2002; Di Emidio 2010, Mazzieri et al., 2010; Bohnhoff and Shackelford, 2013; Malusis and McKeehan, 2013; Bonhoff et al., 2013; Scalia et al., 2014; Razakamantsoa et al., 2016; Scalia et al., 2018; Tian et al., 2019; Chai et al., 2020; Lieske et al., 2020,) or organic molecules (Onikata et al., 1996, 1999; Lo et al., 1997; Fehervari et al., 2016;) have been proposed with the purpose of maintaining low hydraulic conductivity when permeated with aggressive liquids or solutions. Dense prehydrated (DPH) GCLs are particular products obtained by a patented production process which combine prehydration, polymer amendment and densification by vacuum extrusion (Flynn and Carter, 1998). DPH GCLs were shown to preserve low permeability against aggressive permeants (Shroeder et al., 2001, Kolstad et al, 2004; Katsumi et al., 2008; Mazzieri and Di Emidio, 2015) and to have higher chemico-osmotic efficiency coefficients than unamended bentonite (Malusis and Danyarov, 2016). Mazzieri et al. (2013) investigated the permeability and solute retention properties of a conventional needle-punched (C GCL) and a DPH-GCL, which were permeated first with distilled water (DW) and then with an acidic synthetic leachate containing metal cations. After 21.5 pore volumes of permeation with the synthetic leachate, the k of both GCLs increased by about one order of magnitude with respect to permeation with DW, but remained relatively low (3.3×10^{-11} m/s) for the DPH GCL. All metals were retained in both GCLs; however, the DPH GCL retained a larger amount of metals than the C GCL. The retention of metals in the GCLs was ascribed to cation exchange, precipitation of metal solids, and, for the DPH CGLs, also to adsorption of metals by the amending polymers (sodium carboxymethyl cellulose, Na –CMC and sodium polyacrylate, PAAC).

Di Emidio et al. (2017) performed batch sorption tests on kaolin and dredged sediments amended with 2% Na-CMC and found that polymer amendment increased the sorption capacity of the tested soils for Cu and Zn. Wang et al. (2020) prepared a polymer-calcium bentonite composite by pulping, drying and grinding the bentonite with Na (CMC) and sodium hexametaphosphate (SHMP). Characterization by XRD and FTIR showed that these CMC-SHMP-CB composites have a hybrid microstructure from the intercalation of polymer molecules in bentonite interlayers

and exfoliation action during preparation. Modification of CB with CMC and SHMP significantly improved the hydraulic performance as, in the presence of Cd^{2+} and Ni^{2+} cations, the hydraulic conductivity of the composite was 3×10^{-11} m/s, which is much lower than untreated CB. The adsorption capacity values of the composite for Ni^{2+} and Cd^{2+} were 11.01 mg/g and 13.82 mg/g, respectively equal to 5.6 times and 7.2 times the values before modification. Therefore, the amendment significantly improved the adsorption capacity of bentonite for heavy metals. The improvement was ascribed to the complexation of carboxylate (COO^-) groups in CMC with heavy metal cations.

Most of the aforementioned studies have regarded the permeability and/or migration of solutes in GCLs containing conventional bentonite, whereas most studies concerning polymer-amended bentonites have dealt with the hydraulic conductivity or investigated retention of solutes by batch-type experiments. Studies that investigated the permeability and solute retention in polymer-modified bentonites by means of column-type tests (Shackelford and Redmond, 1994) are relatively rare, probably due to the long duration associated to this testing approach in case of very low permeability. With reference to DPH GCLs, the author is not aware of published results of column-type tests where effluent solute concentrations were monitored, except those described in Mazzieri et al. (2013). In that study, relatively high solute concentrations were used, in order to reduce testing times by enhancing the chemical interaction between solutes and bentonite; however, high solute concentrations often result in nonlinear soil-solute sorption behavior, which makes the interpretation of column test results by conventional migration models considering linear equilibrium sorption difficult or inappropriate. In order to facilitate the interpretation of the tests by linear models while allowing comparison with previous results, in the present study the same GCLs used in Mazzieri et al. (2013) where permeated with a solution containing the same solutes (Pb, Zn,Cu), at concentrations within the linear sorption range previously assessed by batch tests (Mazzieri, 2012). Therefore, the purpose of the study was to assess the hydraulic conductivity of the two GCLs when permeated with the dilute leachate with respect to the concentrated leachate. Moreover, the breakthrough of solutes through the

GCLs was monitored, with the purpose to obtain solute transport data to which transport models implementing linear sorption could be applied (transport modeling is however not reported in this paper). The interpretation of the test results was supported by pre-test and post-test X-Ray Diffraction (XRD) analyses and Scannig Electron Microscopy (SEM) observations of the GCLs microstructure.

2. Materials and Methods

2.1 GCLs. The conventional GCL (C-CGL) used in this study is a commercial needle-punched product. It consists of an nonwoven polypropylene cover geotextile (300 g/m^2) and a carrier woven geoteotextile (200 g/m^2), encapsulating a nominal 4200 g/m^2 of powdered natural sodium bentonite. The nowoven cover geotextile is impregnated with additional powdered bentonite (800 g/m^2). The bentonite has cation exchange capacity CEC of 98 meq/100g, with sodium (77 meq/100 g) and calcium (18 meq/100 g) as the main adsorbed cations. Further details on the C GCL are given in Mazzieri et al. (2013).

Dense prehydrated Geosynthetic clay liners (DPH GCLs) are commercial products manufactured by mixing sodium bentonite with a proprietary hydrating solution, which contains the water-soluble polymers Na-carboxymethyl cellulose (Na-CMC), Na-polyacrylate (Na-PAAC) and methanol. The additives are thought to inhibit growth of bacteria and fungi (Schroeder et al., 2001), to increase the workability of the mixture during production and to promote dispersion of bentonite microstructure (Di Emidio, 2010; Wang et al., 2020). The hydrated bentonite mass is then extruded under vacuum into a dense sheet (Flynn and Carter, 1998) and subsequently coupled to geotextiles. The particular product used in this study has a high strength woven polypropylene geotextile (100 g/m^2) and a perforated polyester scrim geotextile (17 g/m^2).

The dried bentonite from the DPH GCL was tested as per ASTM D-7503 for CEC, that was equal to 82.5±2.5 meq/100 g with sodium (62.5 meq/100 g) and calcium (18.0 meq/100 g) as the main adsorbed cations. Further details on the DPH GCL are given in Mazzieri and Di Emidio (2015) .

2.2 Permeant solution. GCLs specimens were first permeated with distilled water (DW) and then with a synthetic solution containing metal cations (Zn^{2+}, Cu^{2+}, Pb^{2+}) as nitrate salts. DW had average electrical conductivity (EC) equal to 0.014 mS/cm and pH equal to 6.2. The synthetic permeant solution, indicated as DSL (Dilute Synthetic Leachate), aimed at representing dilution of a synthetic solution (SL) used in previous studies concerning the same GCLs (Mazzieri, 2012; Mazzieri et al., 2013). The DSL had electrical conductivity *EC* = 2.10 mS/cm, pH=2.8 (average values). The average measured solute concentrations in the permeant solution were $[Cu^{2+}]$=1.39 mM, $[Zn^{2+}]$=1.46 mM, $[Pb^{2+}]$=3.42 mM, $[NO^{-}_{3}]$=14.4 mM. For the sake of comparison, the SL solution used in Mazzieri et al. (2013) had (average values) *EC*=15.3 mS/cm, pH=1.9, $[Cu^{2+}]$=25.6 mM, $[Zn^{2+}]$= 24.6 mM, $[Pb^{2+}]$=24.1 mM, $[NO^{-}_{3}]$=157 mM.

2.3 Permeabily column tests. Permeability tests were carried out in 100 mm diameter flexible-wall permeameter (FWP) as per ASTM D-6676. The GCL test specimens were cut by a sharp knife from the GCL roll. Care was taken to minimize bentonite loss in specimen preparation. The test specimen was placed in the cell, hydrated with DW without gradient for 7 days under an effective isotropic confining stress of 34.5 kPa and then permeated with DW to achieve saturation and determine the reference hydraulic conductivity, k_{DW}. Permeation was conducted by applying a cell pressure of 103.4 kPa and pore pressures of 89.6 kPa and 68.9 kPa (back-pressure) at the inlet and outlet end, respectively. The effective stress level expected in typical applications will in general be higher both in bottom liners of landfills (100-400 kPa) and in base liner of heap leach pads, where ore heights can reach up to 170 m (3200 kPa). In general, the effect of chemical interaction on bentonite performance is mitigated by increasing stress levels; therefore, the results obtained at lower stress are to be considered as conservative with regard to actual stress levels expected in applications (Thiel and Criley, 2005; Anastassopoulos et al., 2009).

Bladder accumulators where used both in the influent and effluent lines throughout the tests. The current height of the specimen, *H*, was calculated from the initial height (H_o) and the measurement of the vertical displacements by means of a

rigid rod connected to a dial indicator. After permeation with DW (1st stage), the permeant liquid was switched to the DSL solution (2nd stage). The pH and EC of the inflow and outflow solutions were monitored during permeation. The outflow solutions were accumulated in the bladder and sampled over regular intervals. The chemical analyses of the influent and effluent solutions for dissolved metals and major ions were carried out by a Dionex ICS 1000 Ionic Cromatograph.

Termination criteria outlined in ASTM D-6676 (scenario 1) were pursued but not fully met for either test. The chemical equilibrium conditions in terms of inlet-to-outlet solute concentration ratio were more closely approached for the C GCL than the DPH GCL, despite the test duration were 340 days (0.93 ys) vs. 1934 days (5.3 ys) for the test C GCL and DPH GCL, respectively.

Due to the effort required and time consumption, no replicate tests were performed. Although this approach does not allow assessing the variability of the test results, it is often adopted in case of time-consuming testing methods. Mazzieri (2012 b) described the results of two column test replicates, similar to those described herein, performed on the conventional C GCL using a multispecies metal solution. After the same number of pore volumes with the metal solution (21.5), the *k* of the two GCL specimens was 1.6×10^{-10} m/s and 7.5×10^{-11} m/s, respectively. The curves of *pH* and *EC* of the effluent solutions vs. the pore volumes of flow were practically coincident. Although the uncertainty of the measurement could not be estimated quantitatively by two replicates only, the experimental method adopted provided consistent and similar results between the two replicates.

2.4 Post-test bentonite analyses. At the end of the permeability tests, bentonite was sampled from the GCLs and examined by X-Ray diffraction. Pre-test and post-test conditions were compared. The bentonite specimens were air dried and sieved through a 75μm aperture sieve before testing. Powdered randomly oriented samples were X-ray analyzed by means of a Philips diffractometer constituted by a PW 1730 generator, a PW 1710 electronic unit, a PW 1050/70 goniometer equipped with proportional counter. Cu kα (Ni filter) radiation (λ = 1.54060 Å) was used under the following conditions: 40 kV, 30 mA, 1°-0.2°-1° slits, a continuous scanning rate of

1°/min, 0.020 step size (2θ), time per step of 1 s and a range of 10^4 c/s (photons per second). Microstructural SEM observations were carried out by a FESEMSUPRA40–ZEISS, Germany (source: Schottky field output–FEG, detector Everhart–Thornley for secondary electrons, 4 sectors solid-state detector for backscattered electrons, maximum voltage: 30 kV). After air drying, the bentonite samples were gilded before the observations by means of an Emitech K550 sputter coater.

3 Results And Discussion

3.1 Macroscopic effects of permeation: permeability and volume change. The hydraulic conductivity, *k*, is plotted versus the net number of pore volumes of flow (Shackelford and Redmond, 1995) *NPV*, in Fig.1a and Fig.1b for the C GCL and DPH GCL, respectively. The pore volume was calculated from the height of the specimen at the end of permeation with DW (H_{DW}).

The values of k_{DW} (Fig.1a) were in the range $(1.0\text{-}2.5)\times10^{-11}$ m/s. During permeation with the DSL, the *k* remained essentially constant or decreased slightly up to *NPV*~10. Gas bubbles were observed in the drainage lines during this stage, likely because of neutralization between HCO^-_3 anions present in the alkaline pore water of the bentonite and H_3O^+ in the acidic permeant solutions, with consequent release of gaseous CO_2. The *k* started to increase gradually until *NPV* ~55 and remained practically constant until *NPV*~75 when the test was terminated (216 days of permeation with the DSL solution). The final *k* was 2.0×10^{-10} m/s.

The results are consistent with those obtained in Mazzieri et al. (2013), where the average *k* of the C GCL permeated with DW under the same effective stress state adopted in this study was 1.5×10^{-11} m/s. Upon permeation with the concentrated synthetic leachate (SL), *k* increased gradually until NPV=5.0 and then remained practically constant to $k \sim 1.8\times10^{-10}$ m/s until NPV=21.5 (94 d of permeation with the SL). Therefore, permeation with SL also increased the *k* of the C GCL by one order of magnitude. However, the increase in *k* was much faster and occurred for a lower value of NPV, due to the higher metal loading. Despite the fact that chemical

equilibrium conditions specified in ASTM D -6676 were not fully met for the test described herein, further increase in *k* values were not expected had the test been continued, since the *k* value was very similar to that obtained on the same GCL permeated with a much more aggressive solution (SL).

The k_{DW} values of the DPH GCL (Fig, 1b) were in the range 7-10×10^{-12} m/s. Upon permeation with the DSL, *k* remained essentially constant, then started to decrease gradually until *NPV* ~9.0 and remained practically constant thereafter at an average value 5.4×10^{-12} m/s. The test was terminated at *NPV*~ 32 (1565 days of permeation). The results indicate that the DPH GCL maintained a lower permeability than the conventional GCL for a considerably longer time, in the presence of the same permeant solution, confirming previous studies (Kolstad et al. 2004; Katsumi et al., 2008). However, unlike the C GCL, the *k* value observed in this study may not be representative of longer permeation times allowing chemical equilibrium conditions to be established.

Mazzieri et al. (2013) observed that the *k* of same DPH GCL to DW was 3.7×10^{-12} m/s (the difference with the k_{DW} measured in this study is thought to be within the experimental scatter. Upon permeation of 21.5 pore volumes with the SL, *k* increased up to about 3.3×10^{-11} m/s (by about one order of magnitude). The chemical equilibrium conditions were more closely approached than in the present study, owing to the higher solute concentrations.

The current height of the specimens during permeation, *H*; is shown in Fig. 1a and Fig.1b for the C GCL (initial height, $H_{o,}$ equal to 5.5 mm) and the DPH GCL (H_o equal to 5.4 mm), respectively. During hydration and permeation with DW, the height of the GCLs increased to 6.75 mm (C GCL) and 10.0 mm (DPH GCL), due to swelling. Therefore, the swell of the DPH GCL was considerably larger than C GCL. Permeation with the DSL solution was associated, for both GLCs, with a decrease in *H* with respect to the stage of permeation with DW.

The increase in *k* and the reduction in volume relative to permeation stage with DW observed for the C GCL is consistent with the migration of divalent metal cations into the GCL. Divalent cations (Pb^{2+}, Zn^{2+}, Cu^{2+}) contained in the synthetic permeant solution substituted monovalent Na^{+} cations on bentonite surface exchange

sites., as confirmed by the measurement of Na^+ concentration in the effluent solution (data not shown). Bentonite retains less water when surface cations are multivalent (Jo et al. 2004), therefore exchange of monovalent cations (Na^+) for divalent (e.g., Pb^{2+}) on the surface sites determines a volume reduction at macroscopic level, as observed in this study. Protons can also replace Na^+ on exchange sites, reduce the swelling volume and increase the hydraulic conductivity of bentonite (Kolstad et al., 2004; Shackelford et al., 2010). However, the concentration of H_3O^+ was about 7.5 times lower than that of divalent cations, therefore the exchange for metals cations likely was predominant.

Recent modeling approaches (Dominijanni and Manassero, 2018; Manassero, 2020) have related the bentonite fabric, intimately linked to its hydraulic conductivity, to a single state parameter, $N_{l,AV,}$ the average number of montmorillonite lamellae per tactoid (aggregate of bentonite platelets). The *k* of bentonite permeated with a given salt solution is determined by the state of flocculation (represented by $N_{l,av}$), which determines the fraction of pore space conductive to fluid flow (micro-void ratio). An increase in *k* upon permeation of a bentonite or GCL with a salt solution is associated to an increase in $N_{l,AV}$. At macroscopic level, flocculation is associated with a volumetric contraction, as observed in this study.

Despite the fact that permeation with DSL induced a volume contraction of the DPH GCL similarly to the C CGCL, the *k* did not increase, rather a significant decrease (by a factor 1.8) with respect to k_{DW} was observed. This result could be explained by the particularly dense and aligned arrangement of bentonite particles determined by calendering under vacuum of the bentonite sheet during production (see section 3.4) and by the effect of the amending polymers which intercalate in the interlayers of montmorillonite lamellae and preserve dispersion of particles. Finally, formation of metal precipitates in the pore spaces of the GCL cannot be excluded. This explanation is also consistent with the lack of breakthrough of metal cations in the effluent solution.

Fig.. 1 Hydraulic conductivity , *k*, (left axis) and specimen height, *H* (right axis)

versus NPV for the C GCL (a) and DPH GCL(b) during permeation with DW (NPV<0) and with the DSL solution (NPV≥0)

3.2 Electrical conductivity and pH. The EC and pH in the outflow solutions are plotted versus *NPV* in Fig. 2 and in Fig. 3, respectively. The outflow EC during permeation with DW reflects the dissolution of accessory salts from bentonite and/or the presence of additives in the case of the DPH GCL. The outflow EC during permeation with the DSL reflects both solute breakthrough and desorption of adsorbed cations from bentonite. For the C GCL, the EC continued to decrease in the early stage of permeation with the DSL ($0<NPV<8.2$) then started to slowly increase. This trend is likely a result of the dominance of residual soluble ions relative to solutes in the DSL during the early stage of permeation. The subsequent increase in EC reflects the gradual breakthrough of solutes. The termination criterion in terms of the outflow-to-inflow EC ratio ($EC_{out}/EC_{in}=1.0 \pm 0.1$) as per ASTM D-6676 was not fully met when the test was terminated.

The effluent EC of the DPH GCL displayed a peak at NPV~ 5, a minimum at NPV~ 17.1 and then an increasing trend. The initial increase in EC mainly reflects the elution of adsorbed Na^+ cations, due to replacement by metal cations, whereas the increase in EC after the minimum reflects also the breakthrough of nitrate from the DSL solution (see 3.3).

Fig. 2. Electrical conductivity in the effluent solution (EC_{out}) of the C GCL and DPH GCL during permeation with DW and with the DSL (EC_{in}=2.1 mS/cm).

For the C GCL, the pH was alkaline (7.3 <pH <8.4) during permeation with DW. Using the DSL ($pH_{in}=2.8$) as permeant, the outflow pH remained practically constant for 0<NPV<15, then gradually declined thereafter to about pH=4 when the test was terminated. Similarly to EC, the termination criteria in terms of the outflow-to-inflow pH ratio ($pH_{out}/pH_{in}=1.0 \pm 0.1$) were not fully met. However, the decrease in pH of the outflow solution is consistent with the partial breakthrough of protons after the initial buffering (neutralization and adsorption of protons by bentonite).

The outflow pH of the DPH GCL during permeation with DW was slightly acidic to neutral (6.2 <pH <7.2); no significant reduction was observed during permeation with DSL. Therefore, the buffering capacity of the DPH GCL was significantly higher than the GCL.

Fig. 3. Effluent pH (pH_{out}) of the two GCLs during permeation with DW and with the DSL solution (pH_{in}=2.8)

.

3.3 Solute breakthrough. The breakthrough curves (C/C_0, where C=outflow concentration, C_0=inflow concentration) of solute species in the permeant DSL solution are plotted in Fig. 4 and Fig. 5, for the CGL and the DPH GCL, respectively. The delay in the breakthrough curve of nitrate in Fig. 4 suggests retardation that can partly be attributed to the dilution of the outflow solution by DW present in the bladder from the first stage of permeation (Mazzieri et al., 2015). However, the dilution effect alone cannot explain the observed delay. A specific test allowed to verify that adsorption of nitrate and metal cations onto the latex membrane used to wrap the specimen was negligible. Under the assumption that the delay was due to adsorption by the bentonite, the mass balance indicated that the unit mass of nitrate sorbed was of 10.4 mg/g of dry bentonite solids.

Some studies have reported no significant adsorption of nitrate to bentonite (e.g., Xi et al., 2010) while others suggest removal capacity of bentonite from aqueous solutions ranging from 8.06 mg/g to 16.05 mg/g (Lazarotou et al., 2020). The difference probably results from different experimental conditions (pH, temperature, initial nitrate concentrations, etc.). A simple sorption experiment was performed to support the interpretation of column test data by mixing and agitating for 48 hours 2 g of bentonite and 100 ml of the DSL (in duplicate). The mixture was then filtered and the nitrate concentration in the filtrate measured. The mass of nitrate removed from the aqueous phase was calculated from the difference between the initial and final average concentrations; the calculated mass of nitrate adsorbed was 18.7 mg/g of dry soil. The test was repeated with 100 mL $NaNO_3$ solution having the same nitrate concentration as in DSL, and no significant adsorption of nitrate was

observed, in accordance with Xi et al. (2010). The main differences between the two tests were the equilibrium pH (5.4 with DSL versus 9.4 with $NaNO_3$) and the presence of metal cations in the DSL. The lower pH may result in protonation of hydroxyl groups on the edge sites of montmorillonite particles, which may promote adsorption of NO_3^- anions (Sposito, 1984).

The attenuation order for metal cations inferred from the delay of breakthrough curves in Fig. 4, is Pb^{2+}>Cu^{2+} >Zn^{2+}. Previous batch tests (Mazzeri, 2012) and test results described in Mazzieri et al. (2013) using the higher concentration solution (SL) showed the same order of retention of metal cations observed in this study. However, owing to higher concentrations in the study by Mazzieri et al. (2013), all solutes (except H_3O^+) achieved complete breakthrough (i.e. C/C_0=1) after 21.5 pore volumes permeated. This allowed to perform a mass balance between the inflow and outflow solutions and determine the mass retained per unit mass of bentonite solids, *S*, (Pb^{2+} =60.7 mg/g; Cu^{2+} =11.6 mg/g; Zn^{2+}=10.3 mg/g). In the present study no metals reached complete breakthrough, therefore only an approximate mass balance was possible: the metals masses retained by the bentonite solids were estimated at the test termination as Pb^{2+} =46.3 mg/g, Cu^{2+} =6.5 mg/g and Zn^{2+}=4.6 mg/g. Gupt et al. (2020) observed in batch sorption tests using a monospecies solution that Pb^{2+} was adsorbed by unamended bentonite following a nonlinear Langmuir isotherm with parameters q_{max}=43.3 mg/g and b=0.04 L/mg. Therefore, the maximum adsorption capacity of Pb^{2+} by the unamended bentonite in a monospecies solution was close to the adsorption capacity value observed in this study using a multispecies solutions. Metals are retained by unamended bentonite via cation exchange, specific adsorption (complexation) and precipitation (Li, 1999; Gu et al., 2010). Desorption of Na^+ and Ca^{2+} in the effluent indicated that cation exchange was an active retention mechanism for metals in the present study. Retention of metals in the solid matrix was confirmed by EDS analyses performed on a small portion of bentonite at the end of the test (see section 3.4).

Fig.4. Solute (NO^-_3, Zn^{2+}, Cu^{2+}, Pb^{2+}) breakthrough curves determined during permeation of the C GCLwith the DSL

For the DPH GCL (Fig. 5), the breakthough of nitrate in the effluent solution clearly occurred at *NPV*=13.5. Therefore, the DPH GCL also displayed retardation of nitrate. A similar explanation as for retardation of nitrate in C GCL can be invoked, with the possible contribution of the much longer retention time of solutes within the DPH GCL, which may have favoured the adsorption phenomena.

All metals cations were retarded; Zn and Cu were detected in the effluent at NPV=19.3, but no significant breakthrough was evident during the test. Desorption of sodium and calcium cations with respect to permeation with DW (Fig. 6) suggests that metal cations were retained in the bentonite by cation exchange. Moreover, amendment of bentonite with the polymers Na –CMC (Wang et al., 2020) and Na-PAC (Chen et al., 2020), has been shown to significantly improve the adsorption capacity of bentonite for heavy metals, owing to the complexation of metals to carboxylate groups. Finally, the porewater of DPH GCL contains relatively high concentrations of phosphate species, likely as a result of SHMP added to the hydrating solution. Fig. 6 shows the concentration of total phosphate (PO_4^{3-}) in the effluent of the DPH GCL during permeation. Precipitation of metal solids (see section 3.4) is also possible as lead, copper and zinc phosphates are all practically insoluble in water. Precipitation of metal solids clogging the pore space would be consistent with the decrease in *k* observed in the early stage of permeation with the DSL (Fig.1). Therefore, the combination of cation exchange, enhanced sorption by polymer treatment and metal precipitation is responsible of the metal attenuation observed for the DPH GCL.

Fig.5. Solute (NO^-_3, Zn^{2+}, Cu^{2+}, Pb^{2+}) breakthrough curves during permeation of the DPH GCL with the DSL

Fig.6. Desorption of major cations and anions during permeation of the DPH GCL with DW and the DSL

3.4 Post-test analyses. Pre-test and post-test powder XRD analyses and SEM observations were perfomed on bentonite extracted from the GCLs to investigate the changes in mineralogical properties and microstructure. The pre-test and post-test diffraction spectra of C GCL and DPH GCL bentonite are shown in Fig. 7a and 7b, respectivey. The diffraction spectrum of pre-test C GCL (unamendend bentonite) shows the typical main reflection at d_{001}=1.25 nm of predominantly sodium bentonite (Miles, 2001) and minor peaks attributed to accessory minerals (quarz, calcite, feldspar, gypsum). The pos-test C GCL spectrum did not change significantly, except for the disappearance of peaks relative to the more soluble minerals (calcite, gypsum), presumably as a result of dissolution by the acidic permeant solution (pH=2.8). In particular, the basal spacing remained practically unaltered, despite the replacement of sodium by heavy metal cations (see section 3.3). Nemeth (2008) found that the basal spacing of Cu- and Pb- adsorbed montmorillonite is 1.3–1.4 nm in case of low metal concentrations and high pH, while in case of high metal concentration and low pH (as in the present study) the basal spacings tend to 1.25 nm (one-layer water arrangement). Nemeth et al.(2005) noted that the characteristic basal reflection of Na-montmorillonite at 1.25 nm is progressively shifted to about 1.45 nm with increasing Zn concentration and decreasing pH .Thus, the basal spacing of post-test unamended bentonite (1.25 nm) is consistent with the predominant occupancy of interlayers by Pb and Cu cations over Zn.

The diffraction spectrum of air-dried pre-test DPH GCL displays distinct montmorillonite peaks, which suggests that the individual units of the clay preserve a well-defined layered structure (Tian et al., 2019). The basal reflection corresponds to a basal distance d_{001}=1.40 nm (Fig. 7b). The increase in the basal distance with respect to unamended Na-bentonite can be ascribed to the intercalation of polymer molecules in the interlayer space of the clay (e.g., Qiu and Yu, 2008). The post-test basal spacing of DPH GCL bentonite further increased to 1.54 nm, which could be due to a partial replacement of Na by metal cations.

Fig.7. Comparison of pre-test and post test powder XRD spectra of C GCL (a) and DPH GCL (b)

SEM migrograph of the bentonites extracted from C GCL and DPH GCL are shown in Fig.8a and 8b, respectively. The pre-test condition of C GCL (left) refers to a water–permeated specimen, whereas the pre-test condition of the DPH GCL refers to the as-received product. In general, C GCL bentonite microstructure presents large randomly oriented aggregates of flaky particles, but no significant differences between pre-test (water permeation) and post test (DSL permeation) conditions are evident. The DPH GCL microstructure presents preferential orientation of particles (Fig 8b –left) and a densely packed arrangement resulting from calendering and vacuum extraction during manufacturing (Mazzieri and Di Emidio, 2015). This microstructure is largely preserved in the post-test DPH GCL (Fig. 8b, right) which is consistent with the observation that the hydraulic conductivity did not increase but rather decreased upon permeation with the DSL. No evidence of polymer strands or webs (e.g., as in Tian et al., 2019) was visible in micrographs even at lower magnification (not shown), reinforcing the hypothesis that polymer-clay interaction occurs in this GCL product in the form of intercalation rather than phase-separated (intact clay particles or aggregates dispersed within a polymer).

Fig.8. Comparison of pre-test (left) and post test (right) SEM micrographs of C GCL (a) and DPH GCL (b).

EDS (Electron Dispersive Spectroscopy) spot-analyses were performed on the same specimens of the two GCLs materials used for SEM observations. The results are shown in Fig. 9. The EDS spectrum of the C GCL (Fig.9a) supports the retention of Pb and Cu, while Zn was not detected. The EDS spectrum of the DPH GCL allowed detecting Cu only. The absence of one or more elements in EDS spectrum may depend upon the limited EDS spot size and nonuniform distribution of retained elements within the specimen. A picture of the upstream surface of the bentonite of

the DPH GCL soon after disassembling the test is shown in Appendix (Figure 10). Since the cover geotextile has no bonding with the bentonite layer, the geotextile was easily peeled off to expose the bentonite surface. Scattered whitish spots can be observed on the bentonite surface, that can be ascribed to precipitated metal solids (lead phosphate, zinc phosphate,) all described as whitish in color in the relevant literature. Further insight into the nature of this spots was not possible due to the difficulty in selectively sampling the very small-sized spots. Similar visual observations were not possible on the C CGL, since peeling off the cover geotextiles would have required cutting the dense network of needle-punched fibers and probably destroying any such evidences.

Fig. 9. Post-test EDS results for C GCL(a) and DPH GCL(b).

4 Conclusions.

Polymer treatment of bentonite is an increasingly adopted approach to improve the resistance of GCLs against chemical attack. The paper compares the hydraulic conductivity, *k*, and solute retention properties of a conventional needle-punched GCL and a DPH GCL, a particular product where polymer treatment and densification are combined to enhance the performance. The two CGLs were permeated with a synthetic electrolyte solution containing Zn^{2+}, Cu^{2+}, Pb^{2+} and NO^{-}_{3}.. The *k* of the conventional GCL increased from 2.2×10^{-11} m/s (water) to 2.0×10^{-10} m/s after 75 pore volumes of permeation with the synthetic solution (215 days). The increase in *k* was associated with the replacement of bound Na^{+} by metal cations and breakthrough of solute species. Conversely, the *k* of the DPH GCL decreased from k=8.9×10^{-11} m/s (water) to 5.4×10^{-12} m/s after 32 pore volumes (1560 days of permeation) with the synthetic solution. The permanence of low *k* likely was favoured by polymer intercalation into the interlayers of montmorillonite and the dense and oriented arrangement of clay particles induced by the manufacturing procedure that was maintained after permeation, as confirmed by SEM imaging. No significant solute breakthrough was observed, except for nitrate. Solute retention in

the GCLs was ascribed to cation exchange, metal solids precipitation and adsorption by polymeric additives in the DPH GCL. The results described in this paper confirmed previous studies showing that the permeability and the containment properties of DPH GCL proved significantly superior with respect to a conventional GCL under a given set of conditions. The contribution of polymer treatment to DPH GCL performance consists in the improvement of workability during manufacturing as well as in the increase in water and solute retention during service life.

5.References

ASTM D6766-20a, Standard Test Method for Evaluation of Hydraulic Properties of Geosynthetic Clay Liners Permeated with Potentially Incompatible Aqueous Solutions, ASTM International, West Conshohocken, PA, 2020, www.astm.org

ASTM D7503-18, Standard Test Method for Measuring the Exchange Complex and Cation Exchange Capacity of Inorganic Fine-Grained Soils, ASTM International, West Conshohocken, PA, 2018, www.astm.org

Athanassopoulos C, Kohlman A, Henderson M, Kaul J, and Boschuk J (2009). Permeability, puncture, and shear strength testing of composite liner systems under high normal loads. In *Proceedings of Tailings and Mine Waste 2009*, Banff, Alberta, Canada.

Ashmawy A, Darwish E, Sotelo N, and Muhammad N (2002). Hydraulic performance of untreated and polymer-treated bentonite in inorganic landfill leachates. *Clays Clay Min.*, **50(5)**, 546-552

Benson CH, Wang X, Gassner FW, Foo DCF (2008). Hydraulic conductivity of two geosynthetic clay liners permeated with an alumina residue leachate. In *Proceedings of the 1st Pan American Geosynthetics Conference & Exhibition, Cancun, Mexico.* Industrial Fabrics Association International (IFAI), Roseville, Minnesota, USA, pp. 94–101.

Bonhoff GL, Shackelford CD, (2013). Improving membrane performance via bentonite polymer nanocomposites. *Appl. Clay Sci*. **86**: 83-98

Bohnhoff GL, Shackelford CD, Malusis MA et al. (2013). Novel bentonites for containment barrier applications. In *Proceedings of the 18th ICSME*, Paris, September, Presses des Ponts

Bouazza A (2002). Geosynthetic Clay Liners. *Geotextiles and Geomembranes* **20 (1)**, 3–17.

Bouazza A (2010). Geosynthetics in mining applications. *In Proceedings of the 6th International Congress on Environmental Geotechnics*, New Delhi, India, vol. 1, pp. 221-259.

Chai J, Prongmanee N (2020)**.** Barrier properties of a geosynthetic clay liner using polymerized sodium bentonite. *Geotextiles and Geomembranes* **48(3)**, 392-399.

Chen Y, Liao R, Yu C, Yu X (2020). Sorption of Pb(II) on sodium polyacrylate

modified bentonite, *Advanced Powder Technology*, **31(8)**, 3274-3286
Di Emidio G (2010). Hydraulic and chemico-osmotic performance of polymer-treated clays. *PhD dissertation*, Ghent University, Belgium, 249 p.
Di Emidio G, Verastegui-Flores RD, Mazzieri F, Dominijanni A (2017). A Modified clays for barriers: a review. *Innovative Infrastructure Solutions*, **2(1)**, 47-60.
Dominijanni A, Guarena N, Manassero M (2018). Laboratory assessment of semipermeable properties of a natural sodium bentonite. *Canadian Geotechnical Journal*, **55(11)**: 1611-1631
Fehervari A, Gates WP, Patti AF et al. (2016). Potential hydraulic barrier performance of cyclic organic carbonate modified bentonite complexes against hyper-salinity. *Geotextiles and Geomembranes* **44(5)**, 748–760
Flynn BN and Carter GC (1998). Waterproofing Material and Method of Fabrication Thereof." United States Patent, Patent Number: 6,537,676 B1.
Gu X, Evans LJ, Barabash SJ (2010). Modeling the adsorption of Cd(II), Cu(II), Ni(II), Pb(II), Zn (II) onto montmorillonite. *Geochimica et Cosmochimica Acta* **74**, 5718–5728
Gupt CB, Bordoloi S, Sekharan S, Sarma AK (2020a) Adsorption characteristics of Barmer bentonite for hazardous waste containment application. *Journal of hazardous materials* Volume 396, 5 September 2020, 122594
Gupt CB, Bordoloi S, Sekharan S, Sarmah AK (2020b). A feasibility study of Indian fly ash-bentonite as an alternative adsorbent composite to sand-bentonite mixes in landfill liner. *Environmental Pollution*. 10.1016/j.envpol.2020.114811.
Jo HY, Benson CH, Edil TB (2004). Hydraulic conductivity and cation exchange in non-prehydrated and prehydrated bentonite permeated with weak inorganic salt solutions. *Clays Clay Min*., **Vol. 52 (6)**: 661–679
Katsumi T, Ishimori H, Onikata M, Fukagawa R (2008). "Long-term barrier performance of modified bentonite materials against sodium and calcium permeant solutions. *Geotext. and. Geomem*., **Vol.26 (1)**, 14–30
Kolstad DC, Benson CH, Edil TB, Jo HY (2004). Hydraulic conductivity of a dense prehydrated GCL permeated with aggressive inorganic solutions. *Geosynt., Intl*., **11 (3)**, 233–241
Lake CB, Cardenas G, Goreham V, Gagnon GA (2007). "Aluminum migration through a geosynthetic clay liner." *Geosynth. Intl*., **14(4)**, 201–209
Lange K, Rowe RK, Jamieson H (2007). Metal retention in geosynthetic clay liners following permeation by different mining solutions. *Geosynth. Intl*., **14 (3)**, 178–187
Lange K, Rowe RK, Jamieson H (2010). The potential role of geosynthetic clay liners in mine waters treatment systems. *Geotext. and geom*, **28 (2)**, 199–205
Lazaratou CV, Vayenas DV, Papoulis D (2020) .The role of clays, clay minerals and clay-based materials for nitrate removal from water systems: A review. *Applied Clay Science*, **185**, 1-18.
Li F (1999). Heavy metal sorption and hydraulic conductivity using three types of bentonite admixes. *Master Th. University of British Columbia*, Canada, 223 p.
Liu W, Gates WP, Bouazza A (2013). Acid induced degradation of the bentonite component used in Geosynthetic clay liners. *Geotextiles and Geomembranes*, **36(1)**, 71–80

Lieske W, Steudel A, Di Emidio G, Baille W(2020) Influence of constitution and mixture treatment of cationic polymers on modified bentonite *Environmental Geotechnics*, **1(1)**:1-9

Lo IMC, Mak RKM, Lee SCH (1997). Modified clays for waste containment and pollutant attenuation. *J. Environ. Eng*., **123 (1)**, 25–32

Malusis, MA, Daniyarov AS (2016). Membrane efficiency and diffusive tortuosity of a dense prehydrated geosynthetic clay liner. Geotextiles and Geomembranes, **44**, 719-730.

Malusis MA, McKeehan D (2013). Chemical compatibility of model soil-bentonite backfill containing multiswellable bentonite. *J. Geotech. Geoenviron. Eng.*, **139(2)**, 189–198

Manassero M (2020). Second ISSMGE R. Kerry Rowe Lecture: On the intrinsic, state, and fabric parameters of active clays for contaminant control. *Canadian Geotechnical Journal*, **57(3)**: 311-336.

Mazzieri F (2012a). Assessment of heavy metals retention in GCLs by column and batch tests. *State of the art and practice in geotechnical engineering GSP 225*: ASCE, Reston/VA: 3447-3456.

Mazzieri F (2012b). Assessment of heavy metals retention in GCLs by column and batch tests. Paper presentation in Technical Session "Hydraulic Properties and Hydrology of Waste Containment Systems at Geo-Congress 2012 *State of the art and practice in geotechnical engineering*; Oakland, CA, March 27, 2012 (in Supplementary Files)

Mazzieri F, Di Emidio G, Van Impe PO (2010). Diffusion of calcium chloride in a modified bentonite: impact on osmotic efficiency and hydraulic conductivity. *Clays Clay Miner*., **58(3)**, 351–363

Mazzieri F, Di Emidio G, Fratalocchi E, Di Sante M, Pasqualini E (2013). Permeation of two GCLs with an acidic metal-rich synthetic leachate. *Geotext. and geomem*. **40 (5)**, 1–11.

Mazzieri F, Di Sante M, Fratalocchi E (2015). Dilution effect of the apparatus on contaminant transport parameters assessed by column testing." *J. Geotech. Geonnv. Engrg.* **Vol. 141 (9)**.

Mazzieri F, Di Emidio G (2015). Hydraulic conductivity of a dense prehydrated geosynthetic clay liner. *Geosynth. Intl*. **22 (1)**, 1-11

Naka A, Flores G, Inui T, Sakanakura H, Katsumi T (2019). Hydraulic performance and chemical compatibility of a powdered Na-bentonite geosynthetic clay liner permeated with mine drainage. *Soils and Foundations* **59**, 1128–1147.

Németh T (2008). Lead and Copper Adsorbed Montmorillonites in Wetting and Drying Cycle .*Revista de la sociedad española de mineralogía, **Vol.9***, 173-174.

Németh T, Mohai I, Tóth M (2005). Adsorption of copper and zinc ions on various montmorillonites: an XRD study. *Acta Mineralogica-Petrographica*, **46**, 29-36.

Miles WJ (2002). Chemical, mineralogical and physical characterization of bentonite for geosyntetic clay liner applications. *Clay Geosynthetic Barriers*, Proc. Int. Symposium Nurnberg, (Zazinger H. et al., eds.), Swets and Zeitlinger, Lesse, pp.129-140.

Onikata M, Kondo M, Kamon M (1996). Development and characterization of a multiswellable bentonite. In *Proceedings of the 2nd Int. Conf. on Env. Geotech.*

(M. Kamon, editor), Balkema, Rotterdam, pp. 587–590.
Onikata M, Kondo M, Hayashi N, Yamanaka S (1999). Complex formation of cation-exchanged montmorillonites with propylene carbonate: Osmotic swelling in aqueous electrolyte solutions. *Clays Clay Min.* **47(5)**, 672-677
Qiu H, Yu J (2008). Polyacrilate/Carboxymethylcellulose modified montmorillonite superabsorbent nanocomposite: preparation and water absorbency. *J. Appl. Polym. Sci.*, **107**, 118–123
Razakamanantsoa AR, Djeran-Maigre I, Barast G (2016). Characterisation of bentonite polymer for bottom liner use. *Env. Geotech.* **3 (1)**, 28–35
Rowe KR, Quigley RM, Brachman RWI, Booker JR (2004*). Barrier systems for waste disposal facilitie*s. 2nd edn. Spon Press, London, 587 pp.
Scalia J, Benson C, Bohnhoff G, Edil T, Shackelford C (2014). Long-term hydraulic conductivity of a bentonite-polymer composite permeated with aggressive inorganic solutions. *J. Geotech. Geoenviron. Eng.*, **140(3)**.
Scalia IV J, Bohnhoff GL, Shackelford CD et al. (2018). Enhanced bentonites for containment of inorganicwaste leachates by GCLs. *Geosynthetics International*, **25(4)**, 392**–**411
Schroeder C, Monjoie A, Illing P, Dosquet D, Thorez J (2001). Testing a factory-prehydrated GCL under several conditions. In *Proceedings of the 8th International Waste Management and Landfill Symposium, Sardinia 2001,* Santa Margherita di Pula, Cagliari, Italy; CISA, Italy: pp.188–196.
Shackelford CD, Redmond PL (1995). Solute breakthrough curves for processed kaolin at low flow rates. *J. Geotech. Engrg*., **121 (1)**, 17–32
Shackelford CD, Sevick GW, Eykholt GR (2010). Hydraulic conductivity of geosynthetic clay liners to tailings impoundment solutions. *Geotextiles and Geomembranes,* **28 (2)**: 149–162
Sposito G.(1984) *The Surface Chemistry of Soils*. Oxford University Press, New York, Oxford,. 234 pp.
Thiel R, Criley K (2005). "Hydraulic conductivity of a GCL under various high effective confining stresses for three different leachates," In *Proceedings of the GeoFrontiers 2005, Waste Containment and Remediation*, Geo-Institute, ASCE.
Tian K, Likos WJ, Benson CH (2019). Polymer Elution and Hydraulic Conductivity of Bentonite–Polymer CompositeGeosynthetic Clay Liners. *J. Geotech. Geoenviron. Eng*.,**145(10)**.
Wang J, Cui M, Su R et al. (2020). Preparation of Modified Calcium Bentonite for the Prevention of Heavy Metal Ion Transport in Groundwater, *Chemical Engineering Transactions,* **81**, 517-522.
Xi Y, Mallavarapu M, Naidu R (2010). Preparation, characterization of surfactants modified clay minerals for nitrate adsorption." *Applied Clay Science* **48 (1)**, 92–96

LIST OF FIGURE CAPTIONS

Fig.1. Hydraulic conductivity , *k*, (left axis) and specimen height, H (right axis) versus NPV for the (a)C GCL and (b)DPH GCL during permeation with DW (NPV<0) and with the DSL solution (NPV≥0).

Fig.2. Effluent Electrical Conductivity (EC_{out}) of the C GCL and DPH GCL during permeation with DW and with the DSL (EC_{in}=2.1 mS/cm).

Fig.3. Effluent pH (pH_{out}) of the of the C GCL and DPH GCL during permeation with DW and with the DSL solution (pH_{in}=2.8).

Fig.4. Solute (NO^{-3}, Zn^{2+}, Cu^{2+}, Pb^{2+}) breakthrough curves determined during permeation of the C GCLwith the DSL.

Fig .5. Solute (NO^{-3}, Zn^{2+}, Cu^{2+}, Pb^{2+}) breakthrough curves during permeation of the DPH GCL with the DSL.

Fig.6. Desorption of major cations and anions during permeation of the DPH GCL with DW and the DSL.

Fig.7. Comparison of pre-test and post-test powder XRD spectra of (a) C GCL and (b) DPH GCL.

Fig.8. Comparison of pre-test (left) and post-test (right) SEM micrographs of (a) C GCL and (b) DPH GCL.

Fig.9. Post-test EDS results for the (a) C GCL and (b) DPH GCL.

Fig.10 (in APPENDIX). Whitish spots on the upstream surface of the DPH GCL at the end of the test (presumably lead and copper phosphate solids)

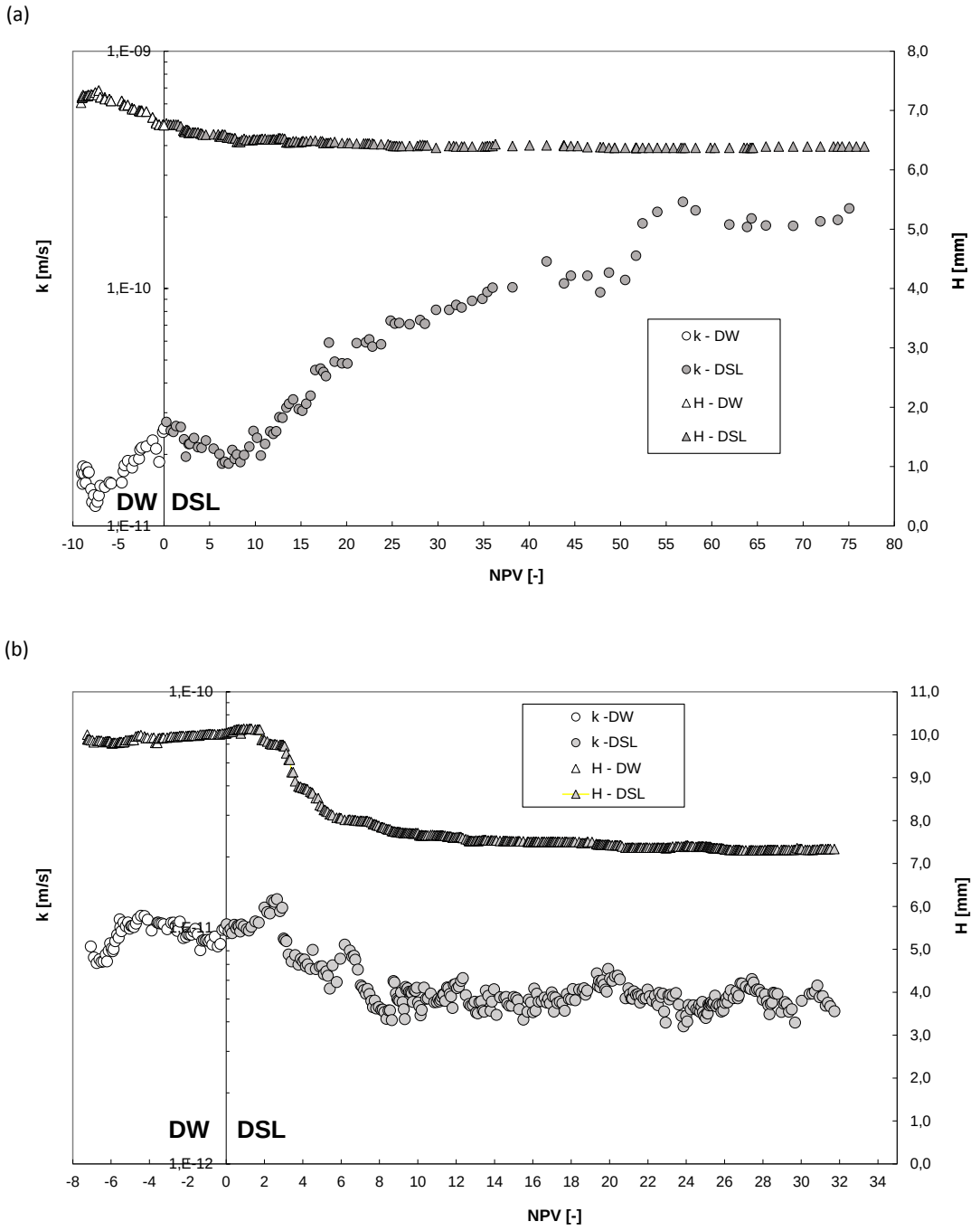

Fig.1. Hydraulic conductivity , *k*, (left axis) and specimen height, H (right axis) versus NPV for the (a) C GCL and (b) DPH GCL during permeation with DW (NPV<0) and with the DSL solution (NPV≥0) .

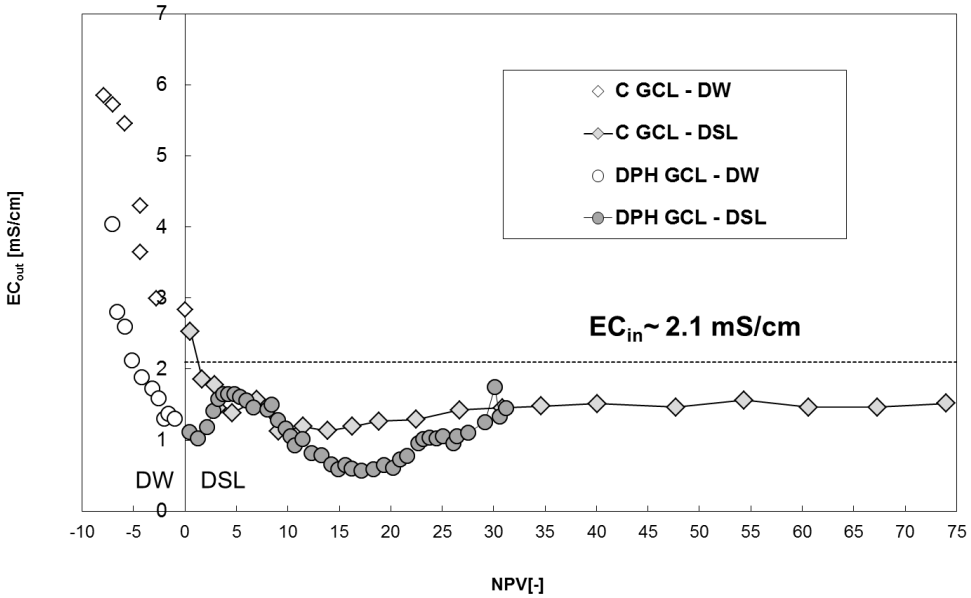

Fig.2. Electrical conductivity in the effluent solution (EC_{out}) of the C GCL and DPH GCL during permeation with DW and with the DSL (EC_{in}=2.1 mS/cm).

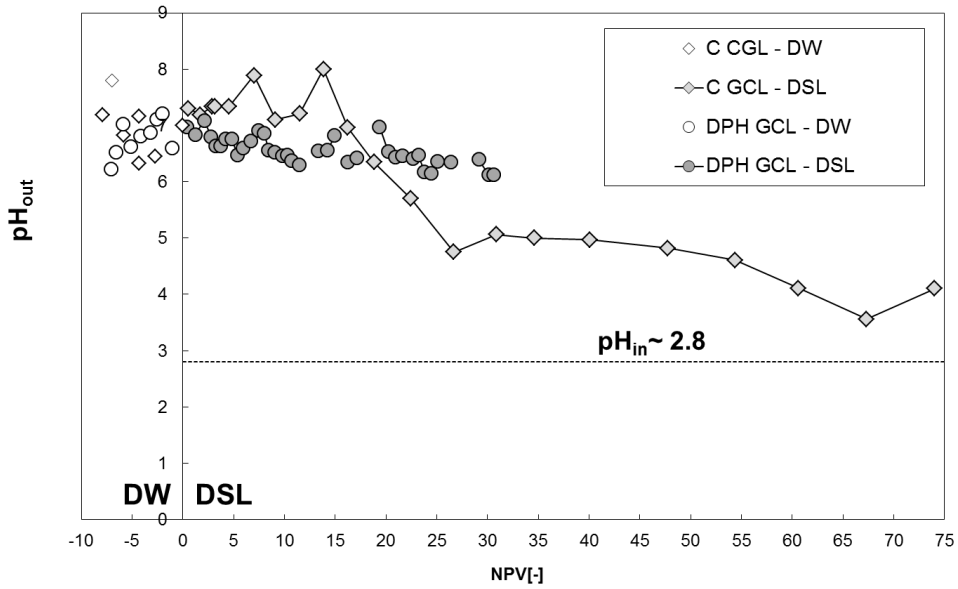

Fig.3. Effluent pH (pH_{out}) of the two GCLs during permeation with DW and with the DSL solution (pH_{in}=2.8)

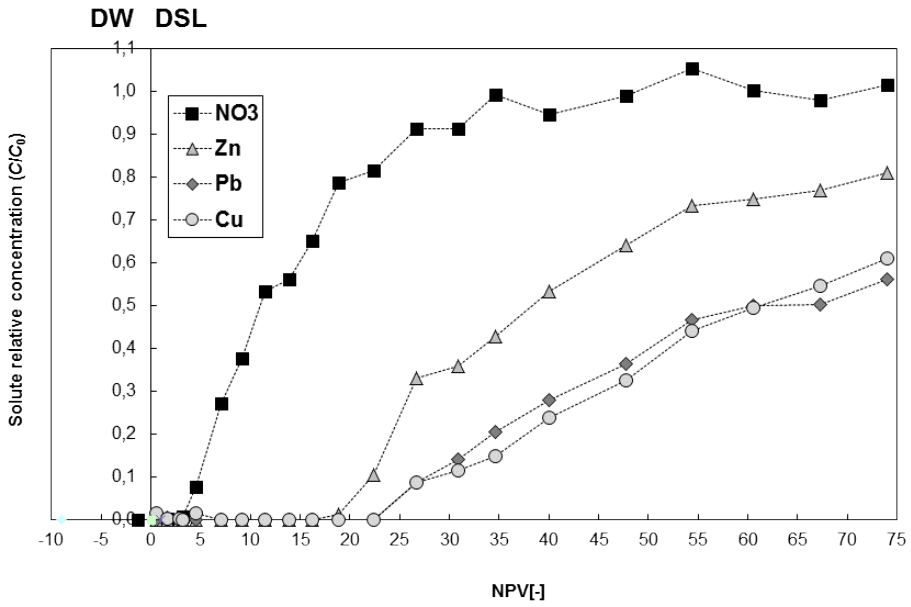

Fig.4. Solute (NO^-_3, Zn^{2+}, Cu^{2+}, Pb^{2+}) breakthrough curves determined during permeation of the C GCLwith the DSL

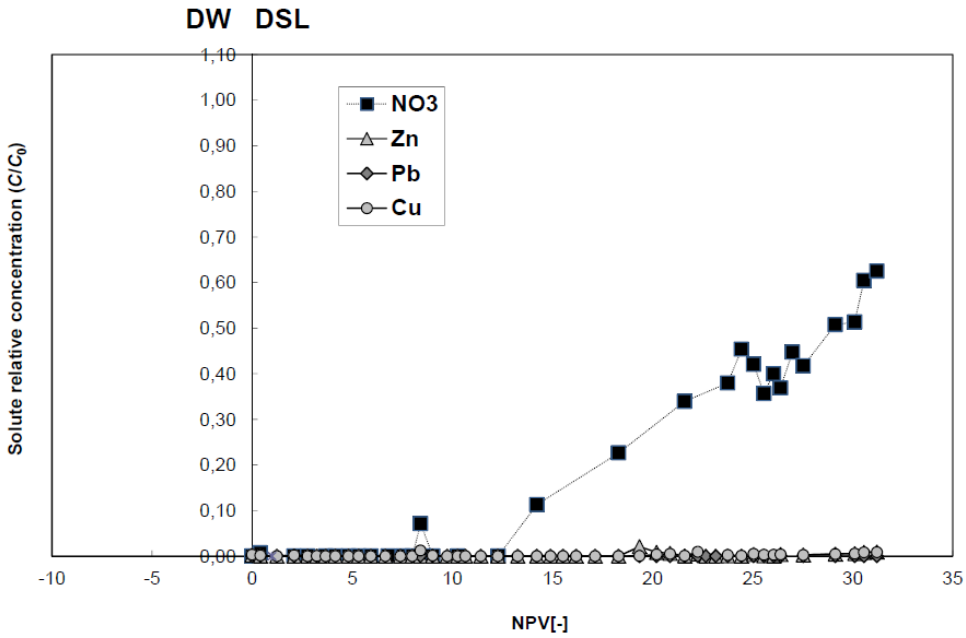

Fig.5. Solute (NO^{-}_{3}, Zn^{2+}, Cu^{2+}, Pb^{2+}) breakthrough curves during permeation of the DPH GCL with the DSL

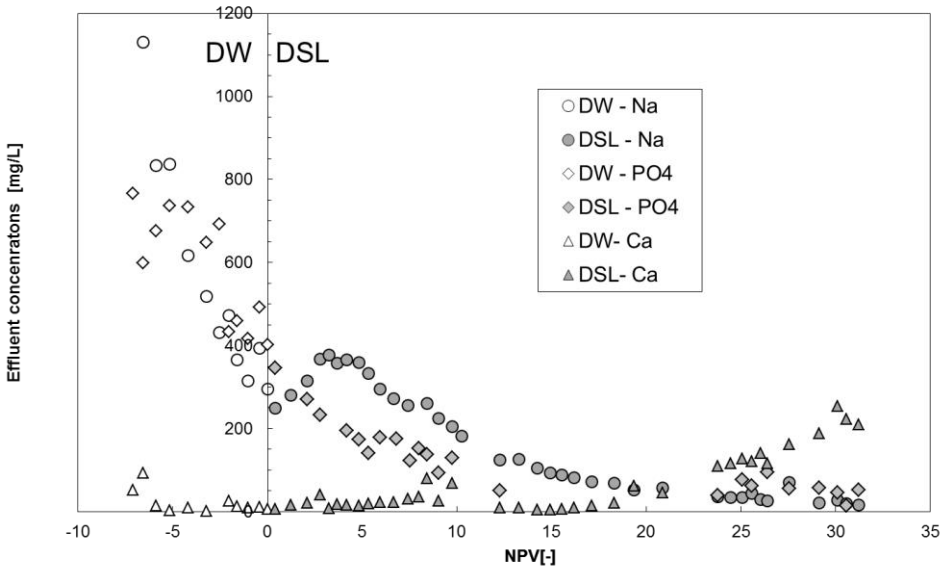

Fig.6. Desorption of major cations and anions during permeation of the DPH GCL with DW and the DSL

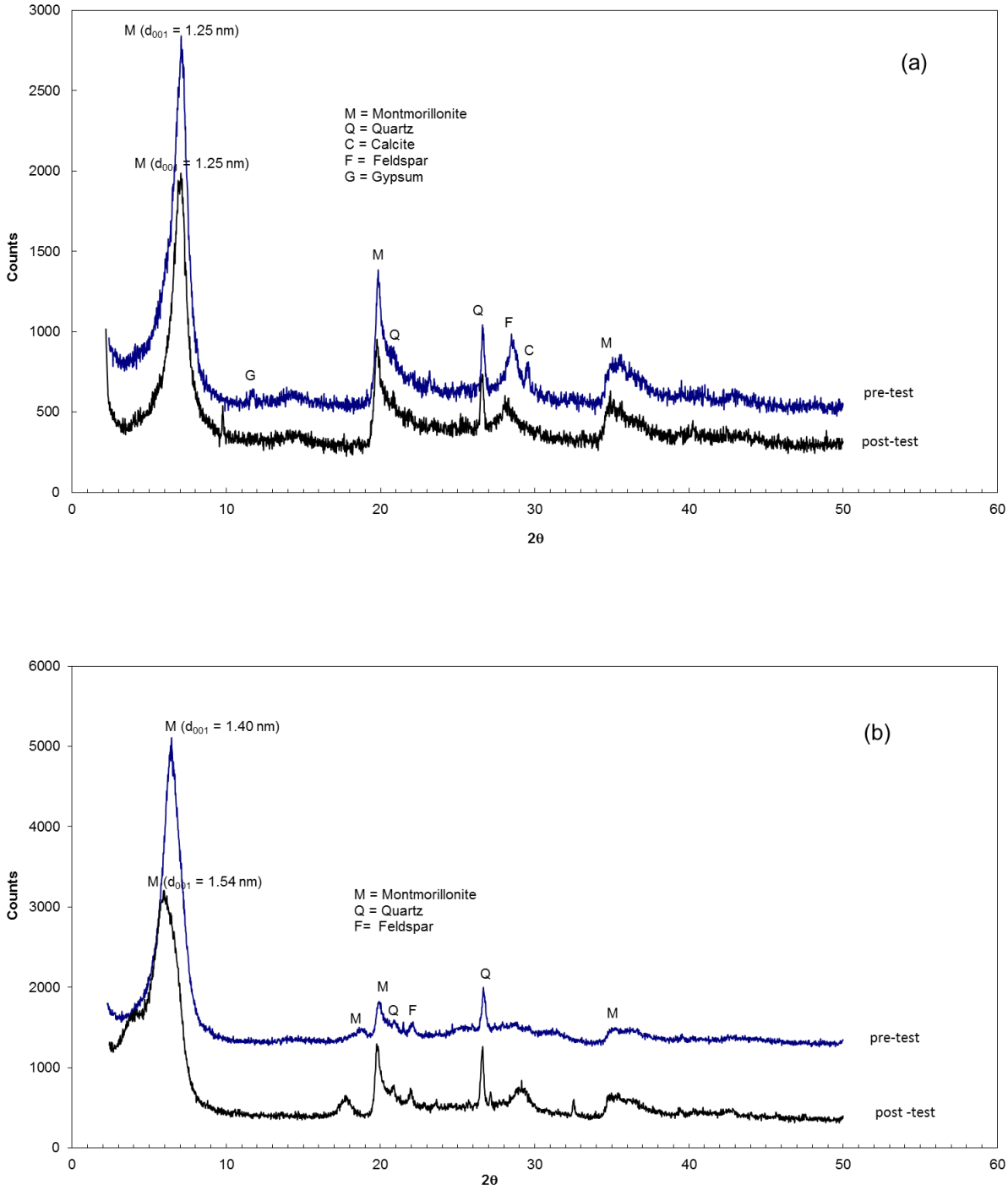

Fig.7. Comparison of pre-test and post-test powder XRD spectra of (a) C GCL (b) and DPH GCL.

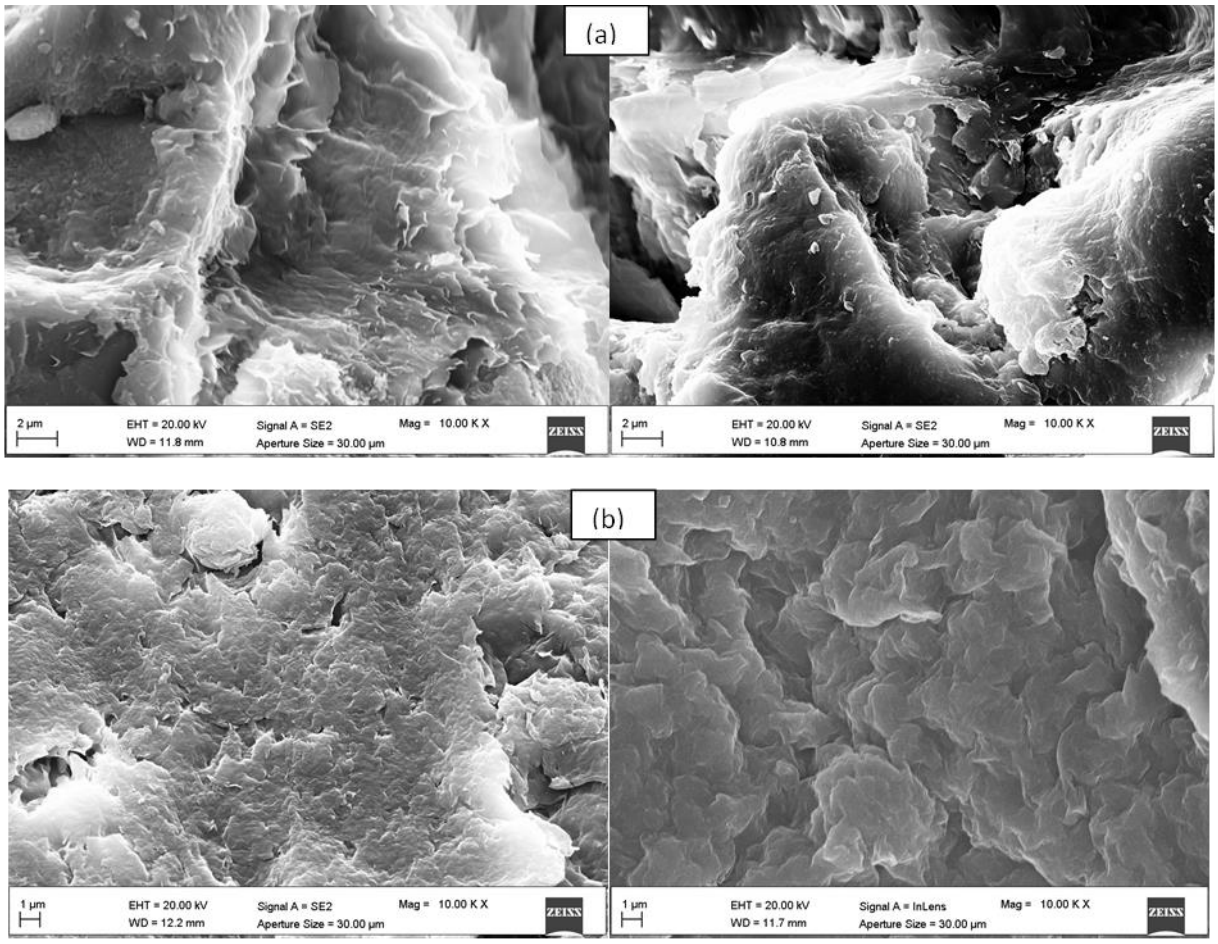

Fig. 8. Comparison of pre-test (left) and post-test (right) SEM micrographs of (a) C GCL and (b) DPH GCL.

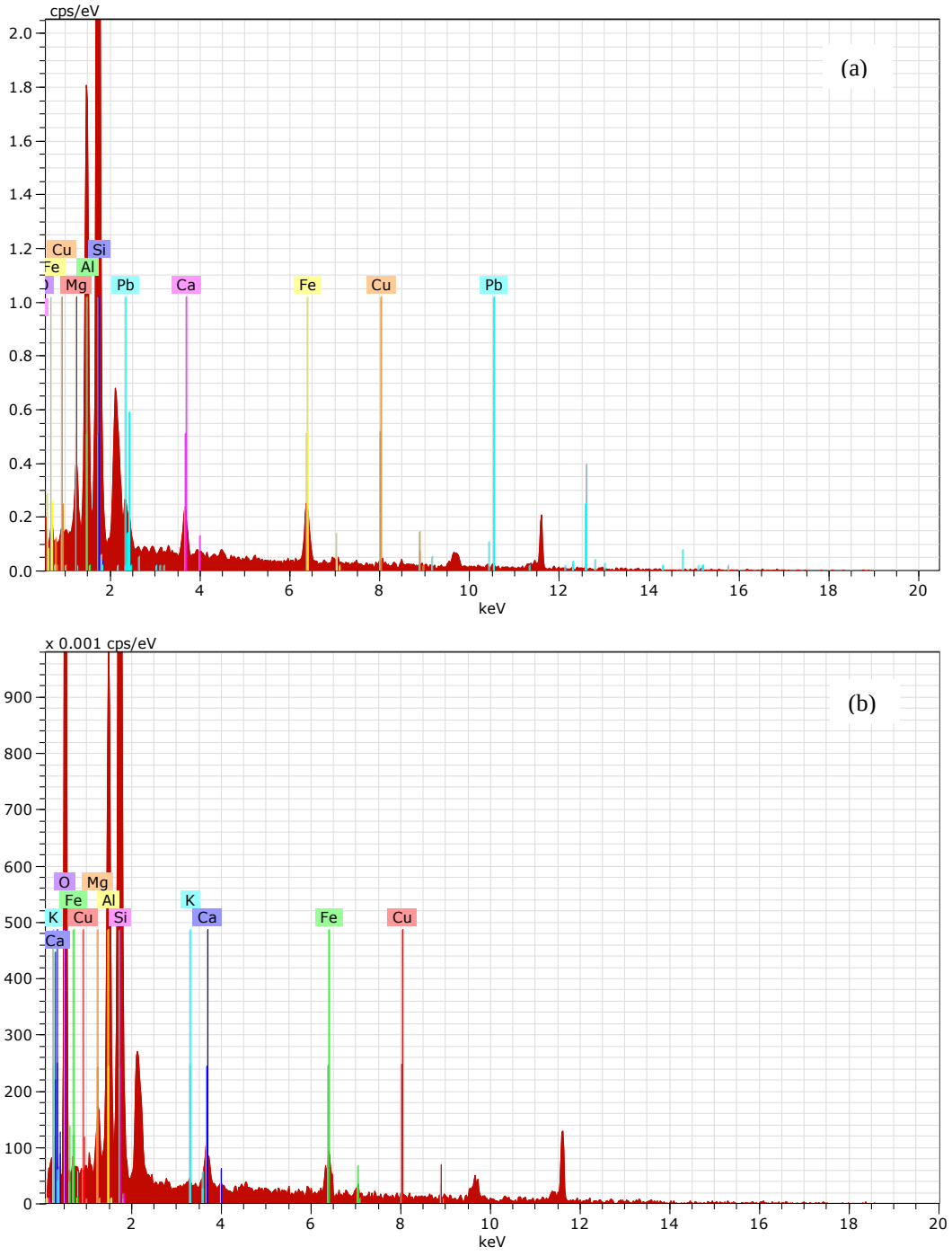

Fig.9. Post-test EDS results for (a) C GCLand (b) DPH GCL.

APPENDIX

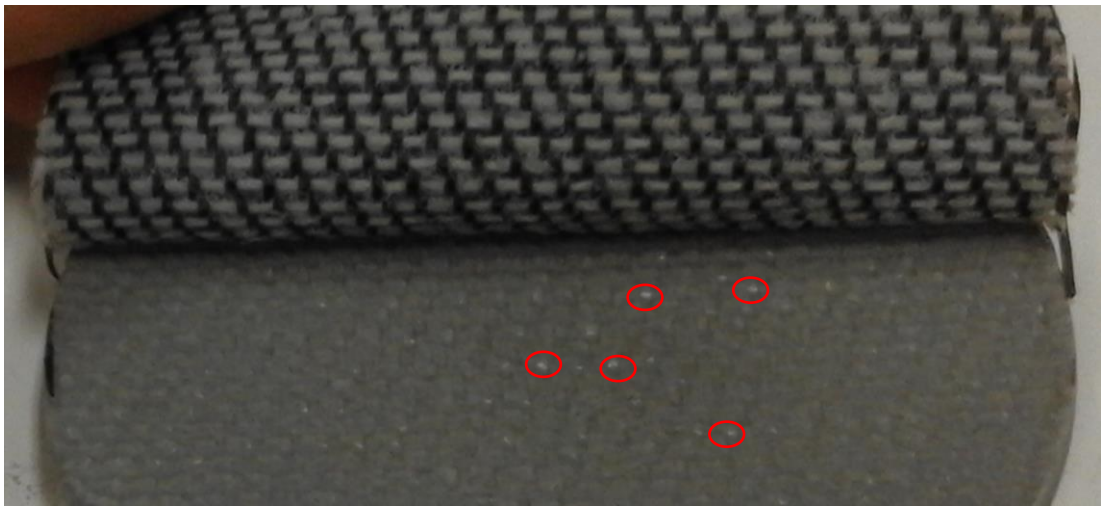

Fig. 10. Whitish spots on the upstream surface of the DPH GCL at the end of the test (presumably lead and copper phosphate solids)